Available online at www.sciencedirect.com
ScienceDirect
Biomaterials 28 (2007) 5176–5184
Biomaterials
www.elsevier.com/locate/biomaterials

Tetanus toxin C fragment-conjugated nanoparticles for targeted drug delivery to neurons

Seth A. Townsend[a,1], Gilad D. Evrony[b,1], Frank X. Gu[c], Martin P. Schulz[e], Robert H. Brown Jr[f], Robert Langer[acd]*

[a]*Department of Biological Engineering, Massachusetts Institute of Technology, 77 Massachusetts Avenue, Cambridge, MA 02139, USA*
[b]*Department of Brain and Cognitive Sciences, Massachusetts Institute of Technology, 77 Massachusetts Avenue, Cambridge, MA 02139, USA*
[c]*Department of Chemical Engineering, Massachusetts Institute of Technology, 77 Massachusetts Avenue, Cambridge, MA 02139, USA*
[d]*Division of Health Sciences and Technology, Massachusetts Institute of Technology, 77 Massachusetts Avenue, Cambridge, MA 02139, USA*
[e]*Institute for Pharmacy and Molecular Biotechnology, University of Heidelberg, Im Neuenheimer Feld 364, Heidelberg 69120, Germany*
[f]*Day Neuromuscular Research Laboratory, Massachusetts General Hospital East, 16th Street, Charlestown, MA 02129, USA*

Received 1 June 2007; accepted 2 August 2007

Abstract

The use of nanoparticles for targeted drug delivery is often facilitated by specific conjugation of functional targeting molecules to the nanoparticle surface. We compared different biotin-binding proteins (avidin, streptavidin, or neutravidin) as crosslinkers to conjugate proteins to biodegradable nanoparticles prepared from poly(lactic-*co*-glycolic acid) (PLGA)–polyethylene glycol (PEG)-biotin polymers. Avidin gave the highest levels of overall protein conjugation, whereas neutravidin minimized protein non-specific binding to the polymer. The tetanus toxin C fragment (TTC), which is efficiently retrogradely transported in neurons and binds to neurons with high specificity and affinity, retained the ability to bind to neuroblastoma cells following amine group modifications. TTC was conjugated to nanoparticles using neutravidin, and the resulting nanoparticles were shown to selectively target neuroblastoma cells *in vitro*. TTC-conjugated nanoparticles have the potential to serve as drug delivery vehicles targeted to the central nervous system.

Keywords: Nanoparticle; Drug delivery; Brain; Cell culture; Nerve; Protein

1. Introduction

Biodegradable polymers, including polylactic acid (PLA) and poly(lactic-*co*-glycolic acid) (PLGA), have been used to create nanoparticles and microparticles that encapsulate a variety of therapeutic compounds over time with favorable safety profiles [1]. Polyethylene glycol (PEG) reduces systemic clearance rates *in vivo* [2], and the functionalization of polymer end groups and subsequent conjugation of targeting moieties (proteins, aptamers, and peptides) permits local drug delivery and reduced systemic toxicity [3]. *N*-hydroxysuccinimide (NHS) and 1-ethyl-3-(3-dimethylaminopropyl)-carbodiimide (EDC) are commonly used for protein conjugation and can generate a stable covalent bond. One problem when using this and other similar techniques is the presence of intermediaries with short half lives, which may lead to inefficient conjugations. In contrast, non-covalent interactions between biotin and its binding proteins (avidin, streptavidin, and neutravidin) are highly specific and do not involve unstable intermediaries. Biotin-binding proteins have previously been used to conjugate proteins to the surface of microparticles and nanoparticles [4–10].

A major challenge in treating neurodegenerative diseases is directly delivering therapies to neurons in the central nervous system (CNS). The CNS is difficult to penetrate

*Corresponding author. Department of Chemical Engineering, Massachusetts Institute of Technology, 77 Massachusetts Avenue, Cambridge, MA 02139, USA. Fax: +1 617 258 8827.
E-mail address: rlanger@mit.edu (R. Langer).
[1]Authors contributed equally to this work.

0142-9612/$ - see front matter © 2007 Elsevier Ltd. All rights reserved.
doi:10.1016/j.biomaterials.2007.08.011

because it is protected by the blood–brain barrier (BBB) [11]. Recently, nanoparticles synthesized from poly(butylcyanoacrylate) with polysorbate 80 [12], and in separate experiments liposomes conjugated to the antibody to the transferrin receptor, have been used to bypass the BBB [13].

Retrograde transport from distal axon terminals to the neuronal cell body is an essential process in neurons; it transports enzymes, vesicles, and mitochondria, and is exploited by viruses and bacterial pathogens as a route to intoxicate motor neurons [14]. It is apparent that retrograde axonal transport of substances from the periphery to motor neuron cell bodies can effectively penetrate the CNS and bypass the BBB [15]. Thus, it may be possible to target nanoparticles to CNS neurons by exploiting retrograde neuronal transport.

One important element in our early studies has been the use of a non-toxic fragment of tetanus toxin, known as tetanus toxin C fragment or TTC [16]. TTC is the neuronal-binding portion of the native tetanus toxin. TTC demonstrates extremely high affinity binding to the neuronal ganglioside $GT1_b$ that is the tetanus receptor, which is located selectively on the surfaces of neurons [17]. Moreover, once TTC binds to neurons, it is readily endocytosed and efficiently carried via retrograde transport from the distal axonal terminus to the neuronal cell body [17,18].

In this report, we compare the ability of different biotin-binding proteins (avidin, streptavidin, and neutravidin) to specifically conjugate a protein to the surface of PLGA-PEG-biotin nanoparticles. We describe the use of TTC-conjugated PLGA-PEG-biotin nanoparticles as a drug delivery system that selectively targets neuronal cells *in vitro*. This system may have applications for delivering therapeutics to neurons affected by neurodegenerative diseases and may allow retrograde transport delivery to the CNS.

2. Methods

2.1. Preparation of PLGA-PEG-COOH and PLGA-PEG-biotin

One gram of PLGA-COOH (20 kDa MW, Lactel Absorbable Polymers) was dissolved in 4 mL dichloromethane and stirred at RT in the presence of NHS (1:8 PLGA:NHS molar ratio) and EDC (1:8 PLGA:EDC molar ratio) to form an amine reactive ester. Unreacted NHS and EDC were removed using a solution containing 70% ethyl ether and 30% methanol. Trace solvents were removed under vacuum for 2 h. The polymer was re-dissolved in 5 mL chloroform and incubated under gentle stirring overnight with HCl.NH2-PEG-COOH (3400 MW, Nektar Therapeutics) or NH2-PEG-biotin (3400 MW, Laysan Bio) (1:1.3 PLGA:PEG molar ratio). *N*-ethyldiisopropylamine (DIEA) was also added to the HCl.NH2-PEG-COOH solution. The polymer was washed with methanol to remove unreacted PEG. The final PLGA-PEG-COOH/biotin product was recovered using ethyl ether, vacuum dried for 2 h, and stored at −20 °C until use.

2.2. NMR analysis

Polymer was dissolved in deuterated chloroform (5–10 mg/mL) and placed in a glass NMR tube. Polymer was analyzed on a Bruker Avance 400 Mhz NMR spectrometer using standard proton NMR to verify PEG conjugation to PLGA. Samples were analyzed for the presence of any intermediary products and to quantify the extent of conjugation.

2.3. Preparation of nanoparticles (nanoprecipitation)

Ten milligrams of PLGA-PEG-COOH or PLGA-PEG-biotin was dissolved in 1.5 mL acetone, and fluorescent nanoparticles were made by also adding 200 μL of coumarin-6 (1 mg/mL in acetone, Sigma Aldrich) [19]. Nanoparticles made of different mixtures of –COOH and –biotin polymers were prepared in the same way, similarly to methods previously described [20]. Five aliquots of 0.3 mL of the polymer solution were continuously injected with a glass syringe to each of five stirring vials of 0.9 mL deionized water to form nanoparticles. The tip of the syringe was submerged during particle formation. The vials were pooled, the acetone solvent was evaporated at RT for 1 h, and nanoparticles were briefly centrifuged (2000 rcf, 10 s) to remove any visible aggregates. Nanoparticles were concentrated and washed to remove any remaining acetone in an Amicon Ultra-4, 100 kDa centrifugal filter (Millipore). Particles were redissolved in a minimal volume of water and stored at 4 °C until use.

2.4. Protein attachment to nanoparticles

Five hundred microliters of nanoparticle solution (~20 mg polymer/mL) was incubated with 2 mL avidin (Invitrogen) solution (2 mg/mL) and gently stirred for 30 min at RT to allow avidin conjugation to the nanoparticles. Neutravidin (Pierce Biotechnology) or streptavidin (Invitrogen) were used analogously for experiments using these as the crosslinker. Nanoparticles were washed and free biotin-binding protein was removed by three centrifugal washes (4000 rcf, 25C, ~10 min) in an Amicon filter. Nanoparticles were resuspended in 500 μL of water, and biotinylated bovine serum albumin (BSA) or TTC (2 mg/mL in PBS) were incubated with the nanoparticles at RT under gentle stirring. Product was washed three times with PBS by centrifugation using an Amicon filter (4000 rcf, 25C, ~20 min) to remove unbound protein. Nanoparticles were resuspended in a minimal volume of PBS and stored at 4 °C until analysis. For all free biotin conjugation experiments, free biotin was mixed with biotinylated TTC in different concentrations, and conjugated analogously. All fluorescent measurements were made on a 1420 VICTOR3 plate reader (Perkin-Elmer) and read in a 96-well plate in triplicate.

2.5. Preparation of BSA–FITC and TTC–FITC

Ten milligrams of BSA was dissolved in PBS (10 mg/mL) or 1 mg of TTC was dissolved in PBS (2 mg/mL), and incubated with EZ-Link NHS–FITC (Pierce Biotechnology) (1–24:1 FITC:protein molar ratio) under gentle stirring for 2 h at RT. Reacted product was collected using a Zeba Desalt Spin Column (Pierce Biotechnology), according to manufacturer's directions.

2.6. Biotinylation of BSA and TTC

Ten milligrams of BSA was dissolved in PBS (10 mg/mL) or 1 mg of TTC was dissolved in PBS (2 mg/mL), and incubated with EZ-Link NHS–PEG_4–biotin (Pierce Biotechnology) under gentle stirring for 2 h at RT. Reacted product was collected using a Zeba Desalt Spin Column (Pierce Biotechnology), according to manufacturer's directions. Biotinylated BSA was incubated at a ratio of 20:1 NHS–PEG_4–biotin:BSA and biotinylated TTC was incubated at a ratio of 10:1 NHS–PEG_4–biotin:TTC in all experiments unless otherwise noted.

2.7. Biotinylation quantification

The extent of BSA and TTC biotinylation was determined using a HABA–biotin quantitation assay (Pierce Biotechnology), according to manufacturer's directions. Briefly, the absorbance of the HABA–avidin

solution was measured at 500 nm.100 μL of biotinylated BSA or TTC was then added to 900 μL of the HABA–avidin solution, and the absorbance at 500 nm measured again. The molar concentration of biotin was calculated from the difference in absorbance after adding biotinylated protein, using a HABA–avidin extinction coefficient of 34,000 $M^{-1} cm^{-1}$. The extinction coefficient for TTC was calculated by measuring the absorbance at 280 nm of a solution of biotinylated TTC whose concentration was measured by a micro BCA assay (Pierce Biotechnology). The absorbance at 280 nm was confirmed to be linearly dependent on concentration using a series of TTC dilutions. The molar concentrations of biotinylated BSA and TTC were determined by measuring the absorbance of the protein solution at 280 nm, and calculated using an extinction coefficient of 43,824 $M^{-1} cm^{-1}$ for BSA [21] and the empirically derived extinction coefficient for TTC. The average number of biotins conjugated to BSA and TTC was calculated as the ratio of biotin concentration to biotinylated BSA/TTC concentration. All absorbance measurements were made on a SpectraMax Plus 384 spectrometer (Molecular Devices) and read in a cuvette in triplicate.

2.8. Nanoparticle characterization and schematic

Nanoparticle size and zeta potential properties were characterized using a ZetaPALS dynamic light scattering (DLS) instrument (Brookhaven Instruments Corporation) as previously described [20]. 3D schematics of the nanoparticle and conjugation system were created using CN3D (NCBI) and 3ds Max (Autodesk) software.

2.9. Flow cytometry

Cells were analyzed using a FACScan flow cytometer (Becton Dickinson) to measure fluorescence (488 nm excitation, 530 and 650 nm emission). Cells were incubated with propidium iodide (5 μg/mL), and cell populations were gated based on forward/side scatter and propidium iodide fluorescence to remove debris and dead cells from analysis. A total of at least 10,000-gated events were obtained for each sample. Data were analyzed using FlowJo software (Tree Star) to generate histograms of each sample.

2.10. Cell culture

N18-RE-105 neuroblastoma, b.End3 brain endothelial, and HepG2 liver cells were grown with previous methods as those previously described [22–24]. Briefly, neuroblastoma cells were cultured in DMEM and supplemented with HAT supplement (100 μM sodium hypoxanthine, 400 nM aminopterin, 16 μM thymidine), 10% FBS, and 1% penicillin/streptomycin. HepG2 and b.End3 cells were grown in MEM and DMEM, respectively, containing 10% FBS and 1% penicillin/streptomycin. All cells were grown in filtered flasks in an incubator at 95% air and 5% carbon dioxide. Media was changed every 48 h, and cells were passaged with EDTA–trypsin when confluent. All media reagents were purchased from Invitrogen. HepG2 and b.End3 cells were purchased from ATCC, and N18-RE-105 cells were a generous gift of Dr. Jonathan Francis at the Massachusetts General Hospital.

2.11. Statistics

An ANOVA analysis was conducted for all multiple point analysis, and a Student's *t*-test was used for all statistical analysis between two groups, unless otherwise indicated. A *p*-value less than 0.05 was considered significant. Results are expressed as mean ± SD unless otherwise indicated.

3. Results and discussion

3.1. Biotin-binding proteins for nanoparticle conjugation

We used biotin-binding proteins to conjugate targeting molecules to the surface of biodegradable nanoparticles for drug delivery (Fig. 1a). The conjugation method uses biotin-functionalized PLGA-PEG polymers and biotin-binding proteins (avidin, streptavidin, and neutravidin) as crosslinkers for conjugation (Fig. 1b) [25–27]. This system has the advantage of conjugating a targeting ligand to the surface of the nanoparticle using highly specific biotin interactions. This may therefore have advantages over other conjugation chemistries that do not distinguish between functional groups that may be present on both the targeting ligand and the encapsulated therapeutic (e.g. primary amines, thiols). Moreover, this system amplifies available protein conjugation sites, because each biotin-binding protein has four biotin-binding sites, and avoids unstable chemical intermediaries present in other protein conjugation reactions. The bonds formed by the biotin interactions are highly stable, and the system can be universally applied to conjugate other targeting molecules with accessible primary amine groups.

3.2. NMR characterization

We prepared PLGA-PEG-biotin polymers by a one step synthesis conducted in anhydrous organic solvents. Proton NMR revealed characteristic peaks of PLGA at 1.5, 4.8 and 5.2 ppm in all PLGA dissolved polymer samples (Fig. 1c–f). Peaks were observed at 3.6 ppm in PLGA-PEG-COOH and PLGA-PEG-biotin, corresponding to the PEG chain (Fig. 1e and f). Using the integration of the relative molecular weights and peaks, the conjugation efficiency of NH2-PEG-COOH and NH2-PEG-biotin to PLGA-COOH was estimated to be approximately 35%. NMR peaks in some samples were detected at 1.2 and 3.4 ppm and identified as residual diethyl ether (Figs. 1d–f). Biotin peaks following conjugation were not easily detected, presumably because the relative biotin signal was masked by the signal from the polymer chain, even when a lower MW PLGA polymer was used (~20 kDa). This has previously been observed in NMR analysis of high molecular weight polymer chains with end-group conjugation [6].

3.3. Protein conjugation to nanoparticles

To show that biotin was functional and present on the surface of the nanoparticles, we synthesized nanoparticles using a solvent/non-solvent nanoprecipitation method and incubated them with avidin–FITC, followed by centrifugal washes. Nanoparticles were made using either PLGA-PEG-COOH or PLGA-PEG-biotin polymers. Nanoparticles formed from either a carboxyl or biotin end group that were not incubated with avidin–FITC showed baseline fluorescence levels in a fluorescent plate reader, whereas nanoparticles incubated with avidin–FITC had significantly higher fluorescence with biotin-functionalized polymer than carboxylic acid controls (Fig. 2a, $n = 5–6$, $p < 0.01$). Subsequent washes reduced but did not eliminate the amount of binding of the avidin–FITC to the

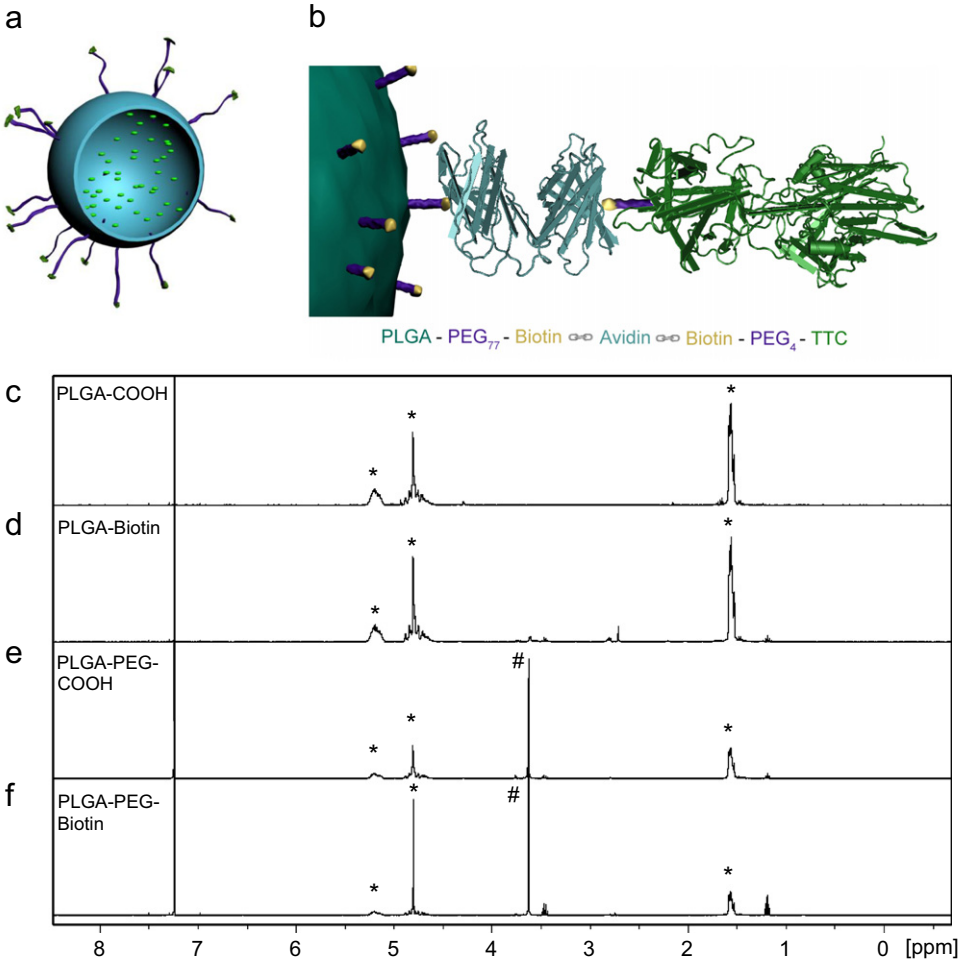

Fig. 1. Protein conjugation to nanoparticles using biotin-binding proteins. Conceptual schematic (not to scale) illustrating (a) the cross-section of a biodegradable polymer nanoparticle that is functionalized with the tetanus toxin C fragment (TTC) and presumed to encapsulate a therapeutic substance, and (b) the conjugation system used to attach functional TTC to the nanoparticle utilizing PLGA-PEG-biotin functionalized biodegradable polymer, and biotinylated TTC with an avidin cross-linker, based on previously published structures [25–27]. Two of the four avidin subunits are shown for illustrative purposes. Proton NMR spectra of (c) PLGA-COOH, (d) PLGA-biotin, (e) PLGA-PEG-COOH, and (f) PLGA-PEG-biotin polymers dissolved in deuterated chloroform. Characteristic peaks are visible for PLGA (*) and PEG (#), but not for conjugated biotin.

PLGA-PEG-COOH, indicating a small amount of non-specific binding, likely a result of electrostatic interactions between the negatively charged polymer and positively charged avidin.

The previous experiments documented that one can conjugate avidin to the surface of a nanoparticle via biotin end-groups. We next tested the possibility that avidin could be used to attach a protein to the nanoparticle. We first conjugated biotin to BSA or TTC in different molar ratios (1:1, 3:1, and 10:1, biotin:protein) and quantified the final number of moles of biotin per mole of protein using a HABA–avidin assay. An empirically derived extinction coefficient of $75{,}550\,\mathrm{M}^{-1}\,\mathrm{cm}^{-1}$ was used for TTC. As predicted, incubation of protein with higher concentrations of NHS–PEG_4–biotin led to higher overall biotinylation (Fig. 2b, ANOVA, $p<0.01$, $n=3$). At 10:1 conjugation ratios, TTC showed higher levels of biotinylation than BSA ($p<0.01$). We therefore used a higher 20:1 molar ratio of NHS–PEG_4–biotin:BSA and quantified the extent of biotinylation. BSA showed slightly higher but not significant biotinylation for 20:1 than for 10:1 ratios (2.2 ± 0.10 vs. 2.0 ± 0.03, ns). For all subsequent experiments, we used protein that was conjugated with a 10:1 biotin:TTC ratio and a 20:1 biotin:BSA ratio.

We then used nonfluorescent avidin and biotinylated BSA–FITC (b-BSA–FITC) to evaluate whether PLGA-PEG-biotin + avidin could be used to conjugate protein to nanoparticles. We incubated nanoparticles with avidin, followed by three washes, and subsequently with biotinylated BSA–FITC followed by three washes (Fig. 2c). Nanoparticles prepared from PLGA-PEG-biotin and subsequently incubated with avidin and biotinylated BSA–FITC gave significantly higher fluorescence than negative controls made from PLGA-PEG-COOH polymers or preparations without avidin (Fig. 2d, ANOVA, $p<0.01$, $n=6$). This suggests that functional biotin is

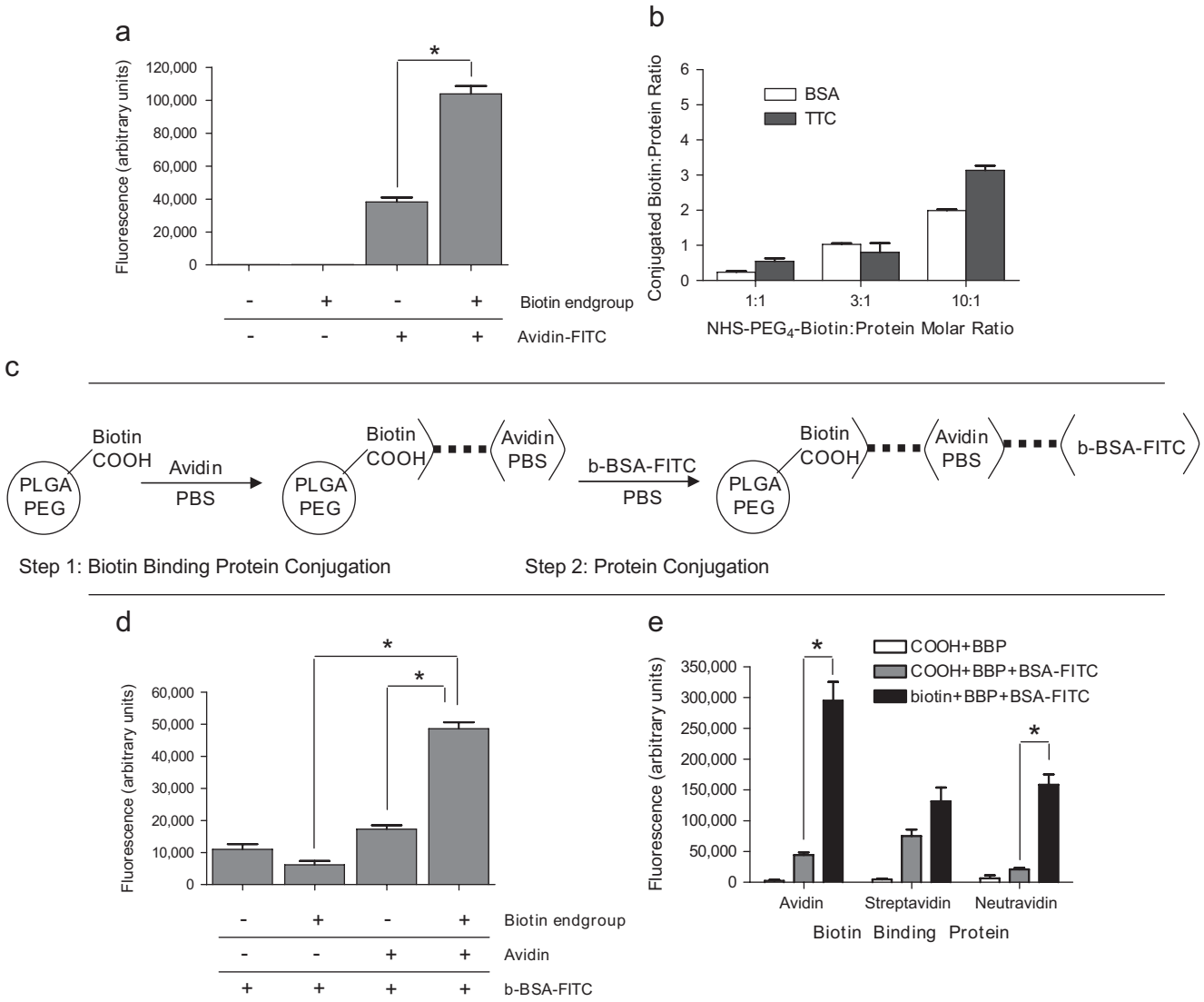

Fig. 2. Protein conjugation to PLGA-PEG-biotin nanoparticles. (a) PLGA-PEG-COOH (−) and PLGA-PEG-biotin (+) nanoparticles incubated with the presence (+) or absence (−) of avidin–FITC and analyzed on a fluorescent plate reader. (b) Quantified extent of biotinylation for BSA (white) and TTC (gray) proteins for different NHS–PEG_4–biotin:protein molar ratios. (c) Schematic representation of overall protein conjugation to PLGA-PEG-COOH or PLGA-PEG-biotin polymer nanoparticles (as indicated). Avidin (Step 1) and biotinylated BSA–FITC (Step 2) were conjugated in sequence to the nanoparticle surface, with PBS washes to remove unbound protein at each step. (d) PLGA-PEG-COOH (−) and PLGA-PEG-biotin (+) nanoparticles incubated with the presence (+) or absence (−) of avidin, subsequently incubated with biotinylated BSA–FITC (b-BSA–FITC) and analyzed on a fluorescent plate reader showing selective protein conjugation to nanoparticles. (e) Comparison of biotin-binding proteins (BBP) as crosslinkers for protein conjugation to nanoparticles. Data are expressed as mean ± SEM. PLGA-PEG-COOH (white, gray) and PLGA-PEG-biotin (black) nanoparticles were prepared and incubated with avidin (left), streptavidin (middle), or neutravidin (right), and subsequently with biotinylated BSA–FITC. Avidin showed the highest overall protein conjugation, whereas neutravidin resulted in reduced non-specific interaction and the most specific protein conjugation.

present on the nanoparticle surface, and that this could be used for protein conjugation. This system could be used as an alternative to NHS/EDC conjugations to avoid unstable intermediaries throughout the conjugation process.

3.4. Comparison of different biotin-binding proteins

In the previous experiments, some non-specific binding of avidin–FITC (Fig. 2a) and biotin–BSA–FITC (Fig. 2d) to the nanoparticle was observed. We predicted that streptavidin (negatively charged) or neutravidin (an uncharged avidin derivative) may reduce non-specific interactions and binding to the nanoparticle. We added each of these three biotin-binding proteins to either PLGA-PEG-COOH or PLGA-PEG-biotin nanoparticles. Biotinylated BSA–FITC was added to nanoparticle preparations after washing out unbound biotin-binding protein. The mean fluorescence was measured on independent preparations in

triplicate using a fluorescence plate reader (Fig. 2e). Nanoparticles with different biotin-binding proteins showed different levels of protein binding (ANOVA, $p<0.01$, $n=3-6$). As predicted, avidin resulted in high levels of overall protein conjugation to PLGA-PEG-biotin nanoparticles, significantly higher than streptavidin ($p<0.01$) and neutravidin ($p<0.05$). Streptavidin and neutravidin fluorescence values were not significantly different. Neutravidin led to relatively high levels of protein conjugation but had lower overall non-specific binding to the nanoparticles than avidin ($p<0.01$). Surprisingly, streptavidin led to non-specific binding to the nanoparticles and observable nanoparticle aggregation (visual observations). These data suggest that avidin has the advantage of generating high levels of conjugated (both specific and non-specific) protein on nanoparticles, whereas neutravidin leads to highly specific protein conjugation to nanoparticles. Neutravidin was used for all subsequent experiments.

3.5. Protein functionality and specificity

TTC in its native form binds with high affinity and specificity to neurons. To test whether conjugation of small molecules to TTC using NHS chemistry affects TTC protein functionality, we conjugated FITC to TTC using NHS-FITC (1:1, 8:1, and 24:1 FITC:protein molar ratios), and incubated the fluorescent protein with N18-RE-105 neuroblastoma cells, which are known to express the ganglioside (GT_{1B}) receptor for TTC. BSA–FITC prepared analogously to TTC–FITC and matched in fluorescence and concentration to TTC–FITC was used as a negative control. In all binding ratios, TTC selectively bound to neuroblastoma cells, whereas BSA did not (Fig. 3a–c). The higher binding of BSA at higher fluorescent ratios may be a result of unbound NHS–FITC that was not removed during protein purification. The double peak observed in TTC binding may be a result of a heterogenous cell population that is observed by light microscopy

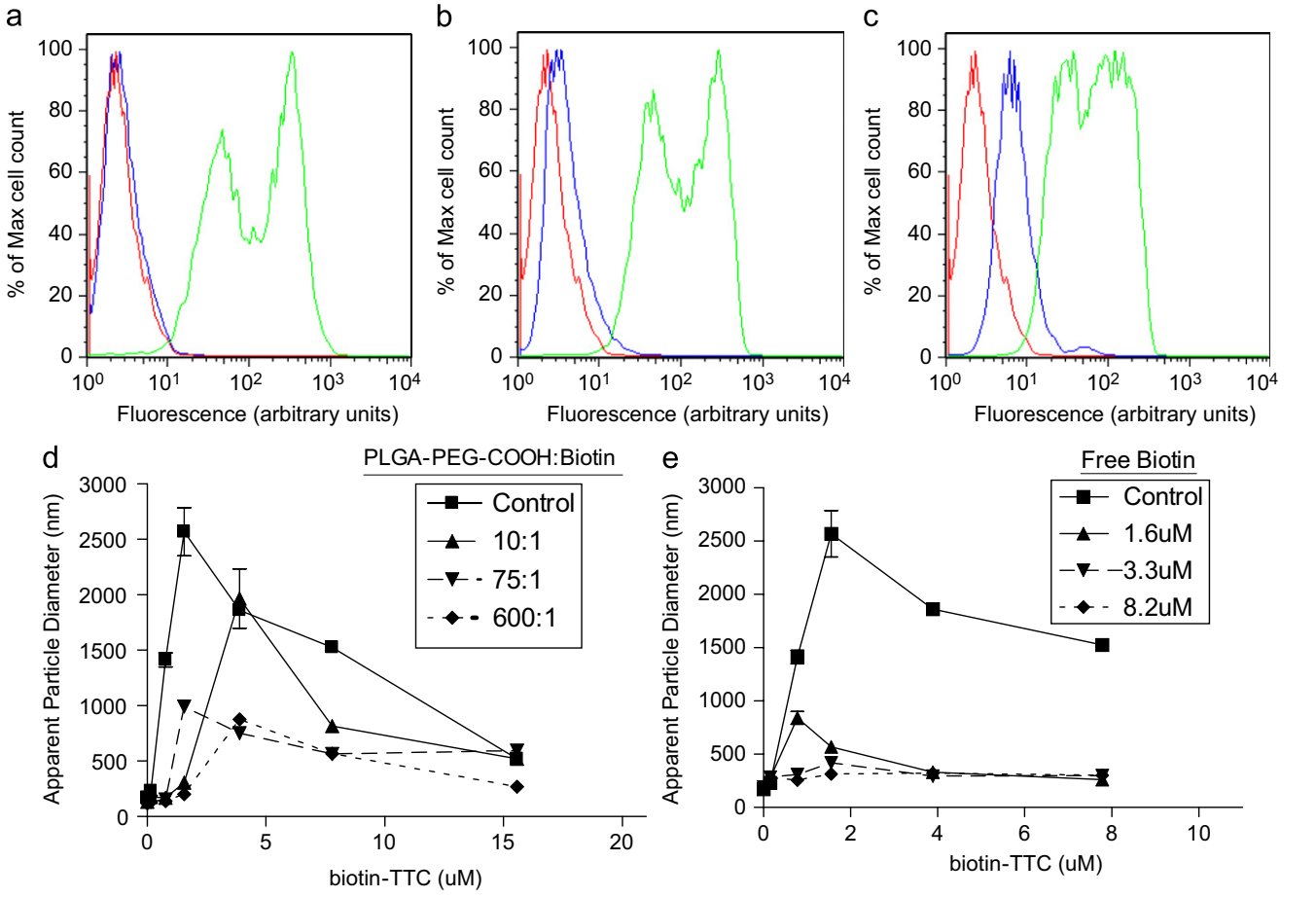

Fig. 3. TTC protein functionality and nanoparticle size optimization. Flow cytometry analysis of N18-RE-105 neuroblastoma cells incubated with fluorescent TTC (green), fluorescent BSA (blue), or PBS control (red), for NHS–FITC:protein conjugation ratios of 1:1 (a), 8:1 (b), and 24:1 (c). TTC remained functional following amine conjugation and preserved its ability to target neurons (a–c). Dynamic light scattering analysis of nanoparticle size following conjugation with neutravidin and biotinylated TTC (d–e). (d) Nanoparticles prepared with different molar ratios of PLGA-PEG-COOH to PLGA-PEG-biotin as indicated (control is 100% PLGA-PEG-Biotin), and (e) free biotin competition with TTC–biotin conjugation to nanoparticles at different concentrations of free biotin as indicated; control is without free biotin. These figures show that nanoparticle aggregation can be reduced by decreasing the number of biotins on the nanoparticle surface (d) or by free biotin competition during conjugation of the biotinylated protein (e). For all sizing experiments, results are expressed as mean ± SD of three independent size measurements of one preparation of nanoparticles.

(visual observations). These data demonstrate that TTC preserves its ability to bind to neurons following amine conjugation.

3.6. Nanoparticle aggregation

In the above paradigm, each nanoparticle binds multiple biotin-binding proteins. Moreover, each neutravidin molecule has four biotin-binding sites. For this reason, nanoparticle cross-linking was sometimes observed in these experiments [28,29]. At least two factors determine the propensity toward aggregation: the ratio of free neutravidin to biotin on the nanoparticle surface in the first conjugation step, and the ratio of biotinylated protein to nanoparticle-bound neutravidin in the second conjugation step. Therefore, we used two approaches to reduce aggregation. The first was to reduce the available numbers of biotin molecules on the nanoparticle surface by creating particles with various mixtures of PLGA-PEG-COOH and PLGA-PEG-biotin in increasing COOH:biotin molar ratios. Nanoparticles prepared from PLGA-PEG-biotin polymers show maximal aggregation at intermediate biotinylated TTC concentrations ($<10\,\mu M$), whereas increasing the PLGA-PEG-COOH molar ratio reduced aggregation at each protein concentration (Fig. 3d). Aggregation was not fully eliminated even at very low PLGA-PEG-biotin concentrations, likely a result of some neutravidin non-specific binding to the nanoparticle surface. The second approach we have used to reduce aggregation is to competitively bind free biotin to neutravidin-binding sites during the biotin–TTC conjugation step. Increasing free biotin reduced aggregation and eliminated aggregation at high free biotin concentrations (Fig. 3e). We again note that increasing concentrations of biotin–TTC also reduced but did not eliminate aggregation. For subsequent experiments, we used $1.6\,\mu M$ free biotin and added TTC in excess of this amount to reduce nanoparticle size, while ensuring that TTC was bound to the nanoparticle surface.

3.7. In vitro cell specificity

We tested the ability of TTC to serve as a targeting protein for specific nanoparticle delivery to neurons. We prepared PLGA-PEG-biotin nanoparticles encapsulating fluorescent coumarin-6 and conjugated TTC to their surface. Neuroblastoma cells were incubated with these nanoparticles as well as negative controls (without both neutravidin and TTC, without TTC, without neutravidin, and with BSA instead of TTC). Cells were analyzed using flow cytometry and shown to be significantly more fluorescent with TTC-conjugated nanoparticles than any negative control (Fig. 4a). Hep G2 liver (Fig. 4b) or b.End3 endothelial cells (Fig. 4c) were incubated with TTC-conjugated or BSA-conjugated (negative control) nanoparticles. Both specific and non-specific uptake ratios are summarized on Table 1. Non-specific binding or uptake was observed in all cell types, which is consistent with previous cell targeting studies using different ligands [30–32]. This is possibly due to background levels of fluorescent nanoparticles that remain after cell washes. Although non-specific binding was observed, non-specific delivery of nanoparticles delivering therapeutic agents alone may not be sufficient for efficacy, necessitating targeted delivery that may increase uptake by specific cell types. The benefit of PEG is most clear in previous *in vivo* studies where PEG has been shown to increase nanoparticle half life by reducing systemic clearance rates [33]. TTC-conjugated nanoparticles showed high selectivity for neuroblastoma cells, indicating that TTC-conjugated nanoparticles may be useful for selective targeting of neurons. Because of the native properties of TTC, these nanoparticles may allow for retrograde transport and

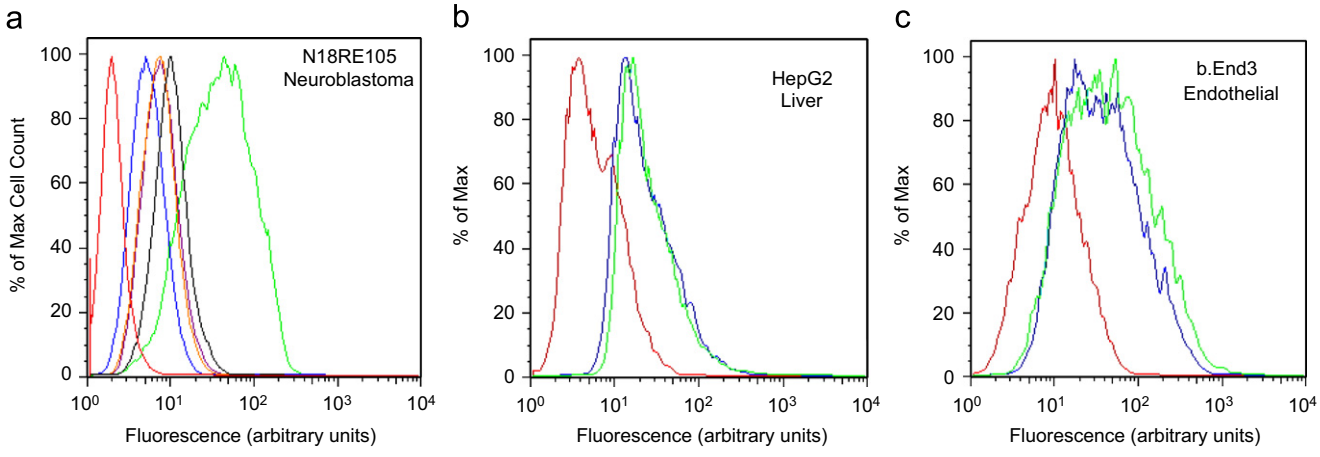

Fig. 4. *In vitro* cell binding of TTC-conjugated nanoparticles. Flow cytometry analysis of N18-RE-105 neuroblastoma (a), HepG2 liver (b), and b.End3 endothelial (c), cells following incubation with TTC-conjugated nanoparticles (green), BSA-conjugated nanoparticles (blue), or a PBS negative control (red). Other negative controls are shown for (a) for nanoparticles without neutravidin (purple), without TTC (orange), and blank nanoparticles (black), demonstrating that TTC-conjugated nanoparticles selectively target neurons.

Table 1
Nanoparticle binding to cells

	N18-RE-105 neuroblastoma	Hep G2 liver	b.End3 endothelial
Non-specific uptake ratio (BSA/PBS)	2.76	4.31	4.99
Specific uptake ratio (TTC/PBS)	25.50	4.87	6.83

Summary of Fig. 4 flow cytometry analysis for N18-RE-105 neuroblastoma, HepG2, and b.End3 cells incubated with TTC or BSA conjugated fluorescent nanoparticles and PBS (negative control). The specific (TTC) and non-specific (BSA) uptake ratios show the fluorescence ratio of conjugated nanoparticles to PBS treated negative controls. Results are expressed as mean fluorescence of each gated live cell population. Each sample represents an analysis of at least 10,000 live-gated cells.

Table 2
Nanoparticle characterization

	Mean size (nm)	Zeta potential (mV)	Polydispersity index
PLGA-PEG-COOH	135.7(1.1)	−32.07(3.19)	0.137(0.023)
PLGA-PEG-biotin	111.1(1.8)	−23.28(1.17)	0.227(0.006)
PLGA-PEG-biotin + NA	144.1(2.4)	−0.497(0.402)	0.198(0.012)
PLGA-PEG-biotin + NA + BSA	175.3(2.3)	−3.37(3.86)	0.226(0.012)
PLGA-PEG-biotin + NA + TTC + free biotin	255.2(6.3)	−5.85(5.00)	0.219(0.007)

Size, charge zeta potential, and polydispersity index for each nanoparticle preparation indicated as determined by dynamic light scattering. Results are expressed as mean (SD) for three size and zeta potential measurements. NA represents neutravidin biotin binding protein.

provide a drug delivery system to specifically target neurons.

3.8. Characterization of nanoparticles

Nanoparticle properties were characterized using DLS to give size, polydispersity, and zeta potential in each preparation (see Table 2). PLGA-PEG-COOH nanoparticles were slightly larger and more negative in zeta potential than those prepared from PLGA-PEG-biotin ($n = 3$, $p < 0.05$). The difference in zeta potential is presumably due to fewer COOH groups in biotin-conjugated nanoparticles. Nanoparticles showed a slight increase in size upon addition of neutravidin, and the addition of the biotinylated protein further increased the size of the nanoparticles.

4. Conclusions

We developed nanoparticles from PLGA-PEG-biotin polymers and used biotin-binding proteins (avidin, streptavidin, or neutravidin) as crosslinkers for protein conjugation. The tetanus toxin C fragment was modified and conjugated to nanoparticles, allowing targeted binding to neuroblastoma cells, while not targeting liver or endothelial cells.

Acknowledgments

We would like to thank Greg Zugates, Benjamin Teply, Erin (Xiaolu) Wei, Jonathan Francis, Etgar Levy-Nissenbaum, Sharon Gerecht, and Glenn Paradis and the MIT Center for Cancer Research flow cytometry core facility for technical guidance. Spectroscopic instrumentation at the MIT DCIF is maintained with funding from NIH Grant 1S10RR13886-01 and NSF Grants CH3-9808063, DBI9729592, and CHE-9808061. This work was supported by funding from the Pierre de Bourgknecht ALS Research Fund, Angel Fund, Project ALS, the Pape Adams Fund, and NIH Grants DE16516 and HL60435. Seth Townsend is supported in part by a National Science Graduate Research Fellowship. Gilad Evrony was supported in part by the John Reed Fund at MIT.

References

[1] Langer R. Drug delivery and targeting. Nature 1998;392(6679 Suppl):5–10.
[2] Pepinsky RB, LePage DJ, Gill A, Chakraborty A, Vaidyanathan S, Green M, et al. Improved pharmacokinetic properties of a polyethylene glycol-modified form of interferon-beta-1a with preserved in vitro bioactivity. J Pharmacol Exp Ther 2001;297(3):1059–66.
[3] Huynh GH, Deen DF, Szoka Jr FC. Barriers to carrier mediated drug and gene delivery to brain tumors. J Control Release 2006; 110(2):236–59.
[4] Nobs L, Buchegger F, Gurny R, Allemann E. Poly(lactic acid) nanoparticles labeled with biologically active Neutravidin for active targeting. Eur J Pharm Biopharm 2004;58(3):483–90.
[5] Nobs L, Buchegger F, Gurny R, Allemann E. Biodegradable nanoparticles for direct or two-step tumor immunotargeting. Bioconjug Chem 2006;17(1):139–45.
[6] Gref R, Couvreur P, Barratt G, Mysiakine E. Surface-engineered nanoparticles for multiple ligand coupling. Biomaterials 2003;24(24): 4529–37.
[7] Cannizzaro SM, Padera RF, Langer R, Rogers RA, Black FE, Davies MC, et al. A novel biotinylated degradable polymer for cell-interactive applications. Biotechnol Bioeng 1998;58(5):529–35.

[8] Weiss B, Schneider M, Muys L, Taetz S, Neumann D, Schaefer UF, et al. Coupling of biotin-(poly(ethylene glycol))amine to poly (D,L-lactide-*co*-glycolide) nanoparticles for versatile surface modification. Bioconjug Chem 2007.
[9] Ben-Shabat S, Kumar N, Domb AJ. PEG–PLA block copolymer as potential drug carrier: preparation and characterization. Macromol Biosci 2006;6(12):1019–25.
[10] Fischer S, Foerg C, Ellenberger S, Merkle HP, Gander B. One-step preparation of polyelectrolyte-coated PLGA microparticles and their functionalization with model ligands. J Control Release 2006; 111(1–2):135–44.
[11] Pardridge WM. Blood–brain barrier delivery. Drug Discov Today 2007;12(1–2):54–61.
[12] Kreuter J. Nanoparticulate systems for brain delivery of drugs. Adv Drug Deliv Rev 2001;47(1):65–81.
[13] Shi N, Zhang Y, Zhu C, Boado RJ, Pardridge WM. Brain-specific expression of an exogenous gene after i.v. administration. Proc Natl Acad Sci USA 2001;98(22):12754–9.
[14] Lalli G, Schiavo G. Analysis of retrograde transport in motor neurons reveals common endocytic carriers for tetanus toxin and neurotrophin receptor p75NTR. J Cell Biol 2002;156(2):233–9.
[15] Kaspar BK, Llado J, Sherkat N, Rothstein JD, Gage FH. Retrograde viral delivery of IGF-1 prolongs survival in a mouse ALS model. Science 2003;301(5634):839–42.
[16] Benn SC, Ay I, Bastia E, Chian RJ, Celia SA, Pepinsky RB, et al. Tetanus toxin fragment C fusion facilitates protein delivery to CNS neurons from cerebrospinal fluid in mice. J Neurochem 2005;95(4): 1118–31.
[17] Shapiro RE, Specht CD, Collins BE, Woods AS, Cotter RJ, Schnaar RL. Identification of a ganglioside recognition domain of tetanus toxin using a novel ganglioside photoaffinity ligand. J Biol Chem 1997;272(48):30380–6.
[18] Sinha K, Box M, Lalli G, Schiavo G, Schneider H, Groves M, et al. Analysis of mutants of tetanus toxin Hc fragment: ganglioside binding, cell binding and retrograde axonal transport properties. Mol Microbiol 2000;37(5):1041–51.
[19] Panyam J, Sahoo SK, Prabha S, Bargar T, Labhasetwar V. Fluorescence and electron microscopy probes for cellular and tissue uptake of poly(D,L-lactide-*co*-glycolide) nanoparticles. Int J Pharm 2003;262(1–2):1–11.
[20] Cheng J, Teply BA, Sherifi I, Sung J, Luther G, Gu FX, et al. Formulation of functionalized PLGA-PEG nanoparticles for in vivo targeted drug delivery. Biomaterials 2007;28(5):869–76.
[21] Fasman DG. Practical Handbook of Biochemistry and Molecular Biology. Boston: CRC Press; 1992.
[22] Malouf AT, Schnaar RL, Coyle JT. Characterization of a glutamic acid neurotransmitter binding site on neuroblastoma hybrid cells. J Biol Chem 1984;259(20):12756–62.
[23] Lewis W, Levine ES, Griniuviene B, Tankersley KO, Colacino JM, Sommadossi JP, et al. Fialuridine and its metabolites inhibit DNA polymerase gamma at sites of multiple adjacent analog incorporation, decrease mtDNA abundance, and cause mitochondrial structural defects in cultured hepatoblasts. Proc Natl Acad Sci USA 1996; 93(8):3592–7.
[24] Piro O, Broze Jr GJ. Role for the Kunitz-3 domain of tissue factor pathway inhibitor-alpha in cell surface binding. Circulation 2004; 110(23):3567–72.
[25] Knapp M, Segelke B, Rupp B. The 1.61 angstrom structure of the tetanus toxin ganglioside binding region: solved by MAD and Mir phase combination. Am Crystallogr Assoc 1998;25:90.
[26] Chen J, Anderson JB, DeWeese-Scott C, Fedorova ND, Geer LY, He S, et al. MMDB: Entrez's 3D-structure database. Nucleic Acids Res 2003;31(1):474–7.
[27] Pugliese L, Coda A, Malcovati M, Bolognesi M. Three-dimensional structure of the tetragonal crystal form of egg-white avidin in its functional complex with biotin at 2.7 A resolution. J Mol Biol 1993; 231(3):698–710.
[28] Costanzo PJ, Patten TE, Seery TA. Nanoparticle agglutination: acceleration of aggregation rates and broadening of the analyte concentration range using mixtures of various-sized nanoparticles. Langmuir 2006;22(6):2788–94.
[29] Costanzo PJ, Patten TE, Seery TA. Protein-ligand mediated aggregation of nanoparticles: a study of synthesis and assembly mechanism. Chem Mater 2004;16(9):1775–85.
[30] Farokhzad OC, Cheng J, Teply BA, Sherifi I, Jon S, Kantoff PW, et al. Targeted nanoparticle-aptamer bioconjugates for cancer chemotherapy in vivo. Proc Natl Acad Sci USA 2006;103(16):6315–20.
[31] Farokhzad OC, Jon S, Khademhosseini A, Tran TN, Lavan DA, Langer R. Nanoparticle-aptamer bioconjugates: a new approach for targeting prostate cancer cells. Cancer Res 2004;64(21):7668–72.
[32] Zhou W, Yuan X, Wilson A, Yang L, Mokotoff M, Pitt B, et al. Efficient intracellular delivery of oligonucleotides formulated in folate receptor-targeted lipid vesicles. Bioconjug Chem 2002;13(6):1220–5.
[33] Gref R, Minamitake Y, Peracchia MT, Trubetskoy V, Torchilin V, Langer R. Biodegradable long-circulating polymeric nanospheres. Science 1994;263(5153):1600–3.